Impact Ionization Noise in SiGe HBTs: Comparison of Device and Compact Modeling With Experimental Results

Paulius Sakalas, Mindaugas Ramonas, Michael Schröter, *Senior Member, IEEE*, Christoph Jungemann, *Senior Member, IEEE*, Artur Shimukovitch, and Wolfgang Kraus, *Senior Member, IEEE*

***Abstract*—The noise behavior resulting from impact ionization (II) was investigated at room temperature for silicon–germanium (SiGe) heterojunction bipolar transistors with box Ge profile ("true" HBTs), featuring a maximum transit frequency of $f_T = 80$ GHz. Noise parameters (NPs) were measured over a wide range of collector–emitter voltages. Modeling was performed using a generalized hydrodynamic (HD) device simulation with a local temperature approach for avalanche generation, drift-diffusion (DD) simulation with a local field model, and the compact model (CM) HICUM/L2 with a conventional local field Chynoweth's law for avalanche generation. Local temperature model parameters were calibrated by matching the avalanche multiplication factor (M) to results obtained from full-band Monte Carlo (MC) simulations. The spectral density of II current noise, obtained from the CM, is in fair agreement with the HD model. Verification of NPs ($NF_{\min}$, R_n, and Γ_{OPT}), obtained with compact and HD model, against experimental values proved that the weak avalanche model is accurate enough to capture II noise in investigated SiGe HBTs.**

***Index Terms*—Avalanche multiplication factor, HICUM, impact ionization (II), noise parameters (NPs), silicon–germanium (SiGe) HBT.**

I. Introduction

BiCMOS TECHNOLOGY with high-performance silicon–germanium heterojunction bipolar transistors (HBTs) has turned into a cost-efficient solution for high-frequency high-volume applications [1]. Present SiGe HBTs have been demonstrated with transit and oscillation frequencies above 300 GHz (see, e.g., [2]–[6]). Future wireless communication electronics, such as radar and millimeter-wave imaging, demand even higher speed in combination with low power consumption and low-cost fabrication. Higher operating frequencies in HBTs can be achieved, among other measures, by increasing the collector doping, which in turn increases the operating collector current density. However, high collector doping results in higher electric fields at the collector–base junction, leading to a reduction in collector–emitter (CE) breakdown voltage (BV_{CE0}). Circuit designers usually are trying to avoid device operation at impact ionization (II) bias conditions, where device output conductance is rapidly increased as well as noise is degraded. Nevertheless, in certain applications, such as fiber optics (with input from photodiode) [7], drivers for optical modulation [8], and RF amplifier designs, transistors may be pushed to operate at voltages beyond BV_{CE0} [9], [10]. Note that we are talking not about transistor in the LNA, operating intentionally in the strong II region, but either unintentionally in the weak-to-medium II region during (automated) optimization (CAD issue) or intentionally at as high V_{CE} as possible for maximum speed. The higher V_{CE} means generally higher maximum transconductance and, thus, gain. Operating voltage can be increased by using an external base resistor, which enables reliable operating conditions at V_{CE} beyond BV_{CE0} [10]. In such a way, output power can be significantly increased since output power is proportional to V_{CE}^2. The maximum speed versus noise tradeoff is important in applications using technologies that have to be exploited up to their limits in order to get working circuits with high performance. Noise can increase due to random II events, which are still not observed from $I(V)$ characteristics, even at V_{CE} below BV_{CE0} [11]. This, however, leads to degradation of the transistor noise performance due to II noise, which was shown to be important for high-speed SiGe HBTs in [11]–[13]. Experimental results indicate a strong increase of the transistor noise figure for a V_{CE} beyond BV_{CE0} [11], [13]. This additional noise is induced by the random nature of the II events and their influence on collector current.

The most accurate semiclassical method for carrier-transport-based noise modeling is the solution of the Boltzmann transport equation, generally using Monte Carlo (MC) techniques. This method includes details of carrier scattering due to its stochastic nature and inherent noise information. However, generation–recombination processes with large time constants introduce long tails in the autocorrelation functions, making accurate MC simulation of noise computationally very expensive. Therefore, hydrodynamic (HD) and even drift-diffusion (DD) models are attractive and often employed for noise simulation.

Manuscript received May 13, 2008; revised November 5, 2008. Current version published January 28, 2009. This work was supported by the German Research Foundation (DFG). The review of this paper was arranged by Editor J. Cressler.

P. Sakalas is with Dresden University of Technology, 01062 Dresden, Germany, and also with the Semiconductor Physics Institute, 01108 Vilnius, Lithuania (e-mail: sakalas@iee.et.tu-dresden.de).

M. Ramonas is with the Semiconductor Physics Institute, 01108 Vilnius, Lithuania, on leave from Bundeswehr University München, 85577 Münich, Germany.

M. Schröter is with Dresden University of Technology, 01062 Dresden, Germany, and also with the University of California, La Jolla, CA 92093, USA.

C. Jungemann is with Bundeswehr University München, 85577 Münich, Germany.

A. Shimukovitch is with the Semiconductor Physics Institute, 01108 Vilnius, Lithuania.

W. Kraus is with Atmel, 74025 Heilbronn, Germany.

Digital Object Identifier 10.1109/TED.2008.2010578

As an acceptable tradeoff between computational effort and accuracy for advanced technologies, HD simulation has evolved since it includes carrier-transport "history" via the energy balance and transport equation.

Fundamentally, II is a "threshold" effect, since prior to generating electron–hole pairs, carriers must gather sufficient energy through an electric field. DD models and classical theory using the *local* field for calculating II [14] ignore the distance necessary for accumulating this energy ("dead" zone). This leads to an overestimation of the multiplication factor M and the associated noise in advanced transistors where the "dead" zone length can be a significant portion of the high-field collector–base space charge region [15]–[18]. Furthermore, particularly in HBTs, carriers related to the main (transfer) current already have accumulated significant energy when entering the high-field region which, in turn, shortens the length required for II. This process can be described by a history-dependent theory, which yields very good agreement with MC simulated ionization coefficients as well as with measured II noise in short Si and GaAs photodiodes [19].

As mentioned before, the circuit design for high-frequency applications often requires the transistors to be operated at their technology limits. Therefore, compact models (CMs) are needed to accurately describe this bias region, including noise for RF applications. Avalanche current effect in popular CMs, such as VBIC [20] and HICUM [21], is restricted to medium current densities and weak avalanche. MEXTRAM [22] can cover II also at high current densities and includes snap back effect [23]. Nevertheless, snap back and high avalanche current degrade convergence and, therefore, are left optional for specific cases. Considering II noise, critical circuit applications generally operate only at weak II ($M - 1 \ll 1$), and therefore, investigations in this paper were focused mainly on this region using CM local field approach, implemented in HICUM/L2, which was verified w.r.t. dc, ac, and II noise. The purpose of this paper was using physical simulations and experimental data to verify how accurate the weak avalanche-current formulation is in terms of high-frequency behavior and noise in SiGe high-speed HBTs. This paper is organized as follows. Section II provides information on the investigated transistor and briefly discusses the employed models. In Section III, device simulation results are compared to experimental and CM data. Furthermore, the observations are discussed. The results are summarized in Section IV.

II. Device Under Test, Model Description, and Verification

The investigated SiGe n-p-n HBTs were available in a production process described in [24]–[26] and feature a peak transit frequency of 80 GHz with a peak oscillation frequency of 110 GHz at $V_{\mathrm{CE}} = 1.5$ V. On-wafer measurements were performed on light emitter concentration (LEC) transistors ("true" HBTs) with a CBEB contact configuration and emitter area of $A_{E0} = 0.5 \times 20.3\ \mu\mathrm{m}^2$. S-parameters were deembedded using a two-step procedure with dummy "open" and "short" structures [27]. Parasitic noise deembedding due to influence of the pad parasitic network was performed with the correlation matrix technique [28]. CM parameters set was extracted from experimental data and generated from a technology parameter set.

In the investigated HBTs, self-heating (s.h.) occurs at higher current densities and CE voltages. It is described in CM by a single-pole network consisting of a lumped thermal resistance R_{th} and thermal capacitance C_{th}. The values of these elements were determined from transient measurement of I_C with pulse durations from 50 ns to 5 ms. Bias pulse duration of 100 ns was found sufficient for the establishment of isothermal operation of the HBT.

Device simulations were performed with Galene III [29], using its HD and DD formulation. Doping profiles were generated with the help of SIMS measurements and adjusted according to electrical data (i.e., by inverse modeling). Standard physical models were used with all required noise and transport parameters obtained through full-band MC simulation under homogeneous bulk conditions [30]. The II process is included in Galene III using the modified Chynoweth law, in which the dependence of the II coefficient α on the electrical field E is given by

$$\alpha = A \exp\left(-\frac{B}{E}\right). \tag{1}$$

The semiempirical constants A and B are well established for bulk silicon. However, under nonlocal transport conditions, the parameters A and B have to be adjusted [31]. Full-band MC device simulations were used to calibrate these parameters for the investigated HBT. Simplified HD and DD models of the actual transistor (without external parasitics and s.h.) were used to analyze pure II-related noise, allowing to eliminate the impact of s.h. on noise. Finally, the comparisons to CM and measured data were performed with a complete 2-D model (including s.h. and parasitic network). In case of the DD model, E in (1) is the local electric field, while for HD simulations, the local temperature model [32] is used

$$E = \sqrt{\frac{3}{2}\frac{U_{\mathrm{Tc}} - U_{\mathrm{Tl}}}{\mu(T_c)\tau_w(T_c)}}. \tag{2}$$

Here, $U_{\mathrm{Tc}} = k_B \cdot T_c/q$ and $U_{\mathrm{Tl}} = k_B \cdot T_l/q$, with T_c as the carrier (electron) temperature obtained from the HD simulation and T_l as the lattice temperature; k_B is the Boltzmann constant; q is the electron charge; $\mu(T_c)$ is the carrier temperature-dependent electron mobility; and $\tau_w(T_c)$ is the carrier energy relaxation time.

Self-heating was included in device simulation self-consistently, based on a lumped thermal resistance R_{th} (as in CMs). The dissipated power and resulting change in lattice temperature are calculated from the power balance equation

$$\Delta T_l = R_{\mathrm{th}}(V_{\mathrm{CE}} I_C + V_{\mathrm{BE}} I_B) \tag{3}$$

where I_B and I_C are the base and collector currents, respectively, and V_{BE} is the base–emitter voltage. The ambient temperature T_0 is used as a starting value for the first iteration to calculate the terminal currents using the HD or DD model. The updated temperature from (3) is then used for the next iteration,

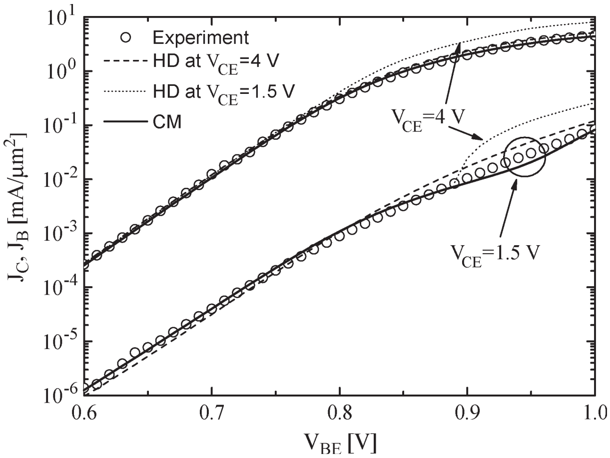

Fig. 1. Forward Gummel characteristics: Comparison between (dashed lines) HD model, (solid lines) HICUM, and (circles) experimental results at $V_{\rm CE} = 1.5$ V. In addition, HD results are inserted for $V_{\rm CE} = 4$ V.

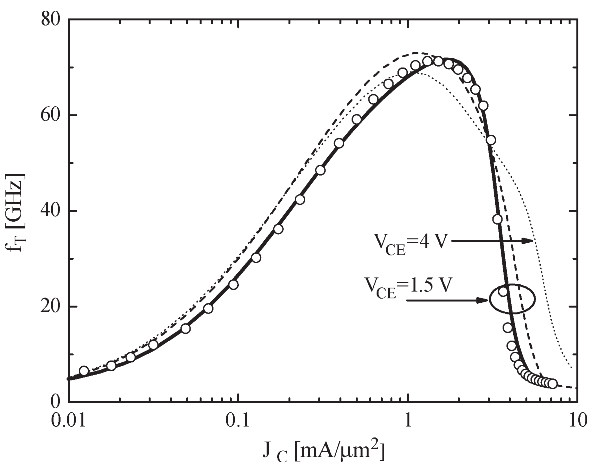

Fig. 2. Transit frequency versus collector current density. Legend as in Fig. 1.

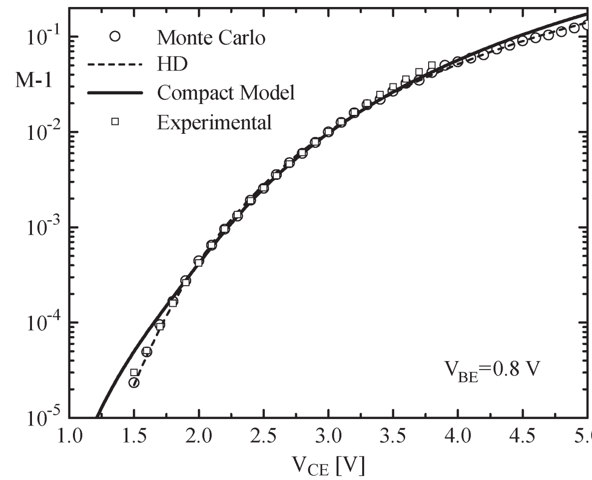

Fig. 3. Avalanche multiplication factor dependence on the applied CE voltage.

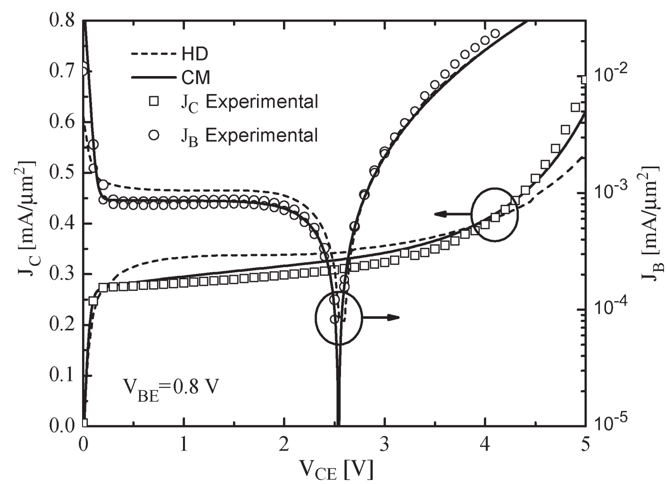

Fig. 4. Base and collector current dependence on CE voltage: (Dashed lines) HD model, (solid lines) HICUM, and (circles) experimental results.

and calculations are continued until the required accuracy is achieved. Model parameters were generated using transistor sizing and model parameter generation tool TRADICA [33] based on an already existing technology file for this production process. A few parameters were slightly recentered (within their process tolerances) to the high-frequency behavior of the investigated transistor. Model verification was then performed for standard characteristics and S-parameters measured in the range of 0.1–50 GHz.

Fig. 1 shows the Gummel plot, and Fig. 2 presents the transit frequency for fixed CE voltages. The minimum value of $NF_{\rm min}$ at low $V_{\rm CE}$ (i.e., at negligible II) was found experimentally to be at $V_{\rm BE} = 0.8$ V and, hence, was used in further noise-related simulations and analysis.

Based on the HD simulation results for standard dc and ac characteristics, the II-related model parameters were calibrated. For this, HD simulations of the HBT were performed first without II. An obtained solution was used as input for non-self-consistent MC simulations. The resulting (electron) avalanche multiplication factor was then employed for adjusting the constants A and B in (1) used for HD simulation. As shown in Fig. 3, excellent agreement is obtained between HD and MC results for $M-1$ over a wide CE voltage range. A similar calibration procedure was performed for DD simulation. Since, avalanche multiplication factor is not directly available in HICUM, it was determined from internal CM variables, namely, $I_{\rm avl}$ and the transfer current $I_T (= I_C)$ according to

$$M - 1 = \frac{I_{\rm avl}}{I_T}. \quad (4)$$

According to Fig. 3, CM, after adjusting the corresponding model parameters, fairly agrees with HD, MC, and experimental results between 1.8 and 4.0 V but starts to overestimate M outside of this range. Experimentally, multiplication factor was measured using forced emitter current method [34]. These discrepancies, which are being further investigated, may be caused by the weak avalanche approximation in CM approach [35] and by the use of a local field. At $V_{\rm CE} \approx 4.5$ V, avalanche generation starts to influence also the collector current. However, as will be shown later, this influence is hardly observable in the noise parameters (NPs).

Fig. 4 shows the experimental and modeled base current densities as a function of $V_{\rm CE}$ at $V_{\rm BE} = 0.8$ V. The holes generated by II are accelerated toward the base and exit through the base terminal. When the hole current due to II exceeds the emitter

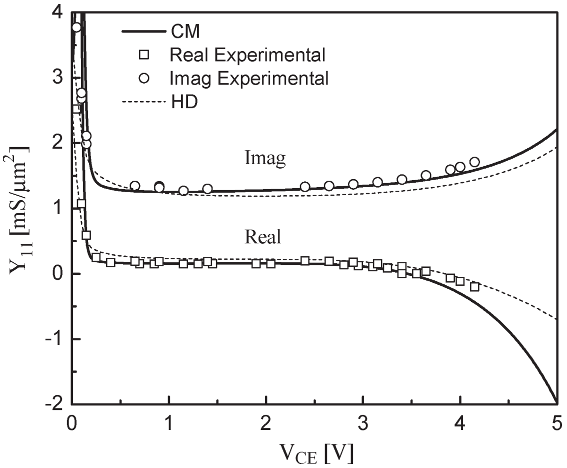

Fig. 5. Real and imaginary parts of Y_{11} versus CE voltage at 8 GHz. Comparison between (dashed lines) HD model, (symbols) experimental results, and (solid lines) HICUM.

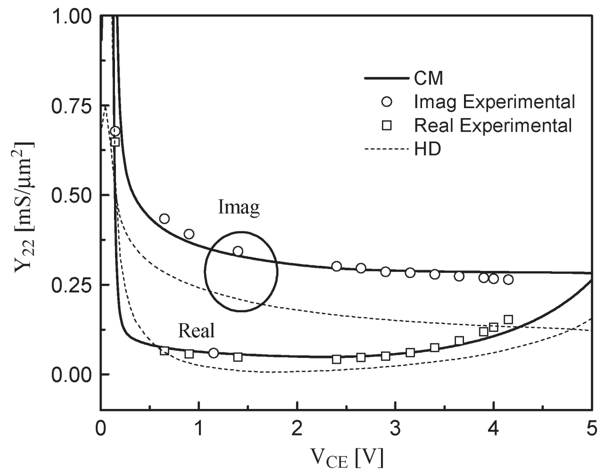

Fig. 7. Real and imaginary parts of Y_{22} versus CE voltage at 8 GHz. Legend as in Fig. 5.

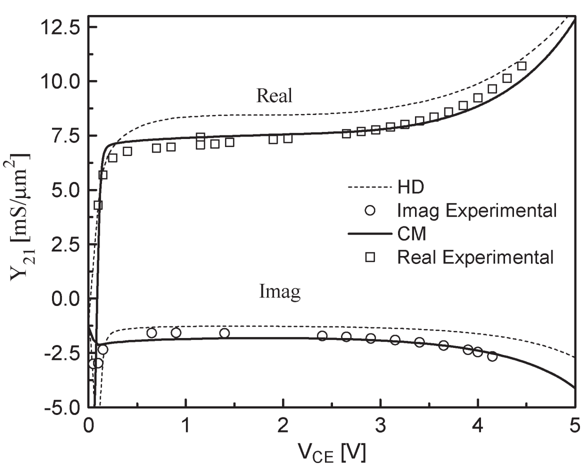

Fig. 6. Real and imaginary parts of Y_{21} versus CE voltage at 8 GHz. Legend as in Fig. 5.

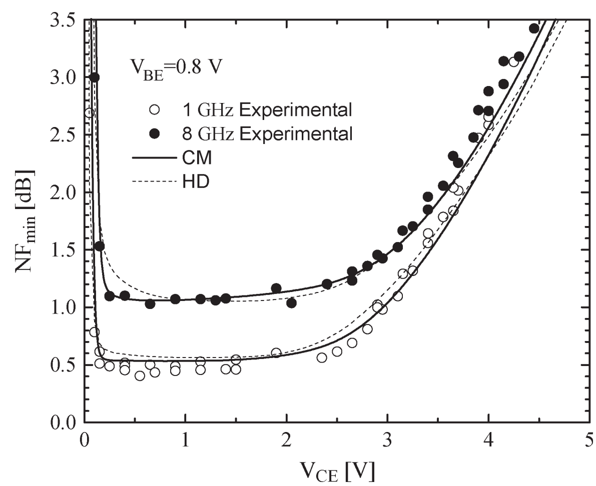

Fig. 8. Minimum noise figure $NF_{\min}$ versus CE voltage: (Dashed lines) HD simulation results with s.h. and II, (solid lines) HICUM, and measurements at (open circles) 1 GHz and (filled circles) 8 GHz, respectively.

back-injection current, I_B reverses its sign (at $V_{\rm CE} \approx 2.5$ V). The breakdown voltage $BV_{\rm CE0} = 2.5$ V is modeled well by both CM and HD simulation. Beyond about 3.5 V, simulation results start to yield a somewhat lower avalanche current than measured, which may be caused by the influence of s.h. and the temperature coefficients used. The corresponding output characteristic is also compared in Fig. 4. As more detailed investigations have shown, the main increase in J_C is caused by s.h. (due to $V_{\rm BE} = $ const). For instance, s.h. at $V_{\rm CE} = 5$ V increases the current density from 0.37 to 0.57 mA$/\mu$m^2 [12].

Since II noise is resolved from $NF_{\min}$ better at lower frequencies [13], Y-parameters and NPs are investigated in more detail for the selected frequencies of 1 and 8 GHz. HD and CM Y-parameters are compared in Figs. 5–7 to experimental data as a function of $V_{\rm CE}$ and for a fixed frequency of 8 GHz only. In particular, for CM, an excellent agreement is obtained here (and also at 1 GHz, which is not shown). A small deviation of HD (2-D case) simulated imag $\{Y_{12}\}$ (not shown in this paper) and imag $\{Y_{22}\}$ is due to omitting parasitic (oxide) and the foreside portions of the capacitances as well as intradevice substrate coupling. However, simulation of the resolved noise sources shows that thermal noise from the substrate resistance ($R_{\rm SU}$ in CM) and shot noise from the collector-substrate diode current, as well as the small change of the transfer function through the parasitic (oxide) and the foreside capacitances, have negligible influence on the NPs in the frequency range $f < 10$ GHz. At higher frequencies, the external capacitances slightly reduce $NF_{\min}$ and affect the optimum source reflection coefficient ($\Gamma_{\rm OPT}$) (cf. Figs. 11 and 12).

For HD noise simulations, the Langevin noise model [36], implemented in Galene III, was used. Relevant physical effects, such as electron and hole scattering in the conduction and valence bands, Shockley–Read–Hall recombination, and II were included.

III. Noise-Related Results and Discussion

The standard NPs as a function of $V_{\rm CE}$ at the selected frequencies of 1 and 8 GHz are shown in Figs. 8–10. According to Fig. 8, the $NF_{\min}$ is fairly constant between 0.2 and 2.5 V but increases rapidly below 0.2 V and beyond 2.5 V. In these regions, the curves for different frequencies tend to merge. The $NF_{\min}$ increase at low $V_{\rm CE}$ is due to the gain

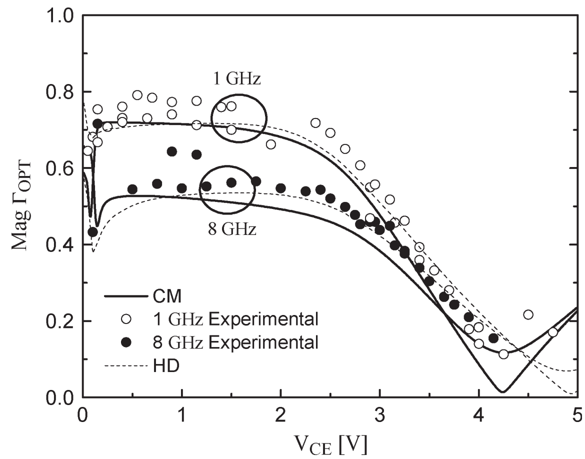

Fig. 9. Magnitude of optimum source reflection coefficient Γ_{OPT} versus CE voltage. (Dashed line) HD simulation results with s.h. and II, (solid line) HICUM, and (scattered line) measurements.

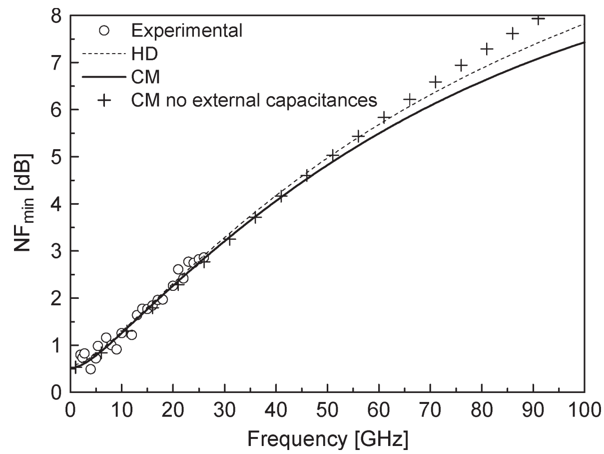

Fig. 11. $NF_{\min}$ versus frequency at $V_{\mathrm{CE}} = 1.0$ V and $V_{\mathrm{BE}} = 0.8$ V. Measured data were obtained with ATN system.

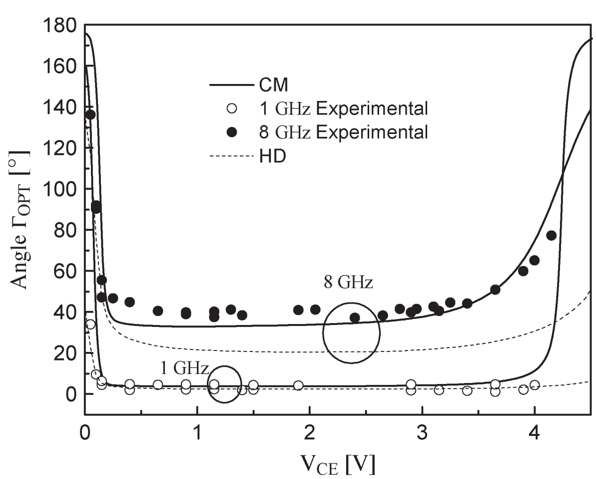

Fig. 10. Phase of optimum source reflection coefficient Γ_{OPT} versus CE voltage. Legend as in Fig. 8.

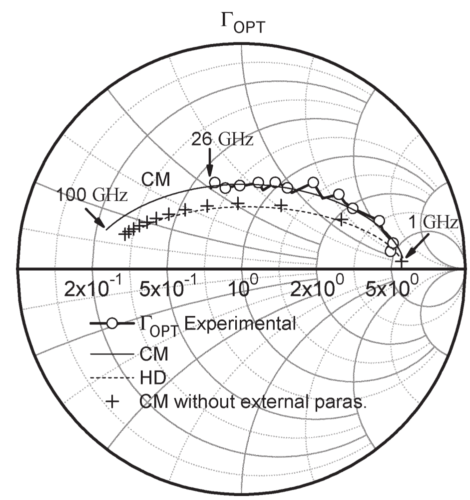

Fig. 12. Γ_{OPT} versus frequency at $V_{\mathrm{BE}} = 0.8$ V. (Dashed line) HD simulation, (solid line) complete HICUM, (crosses) HICUM without external parasitic capacitances and substrate network, and (scattered line with open symbols) measured data.

drop (cf. Figs. 5 and 6). More detailed investigations of s.h. impact, performed with HD model, revealed that, although s.h. considerably increases the collector terminal current, its impact on $NF_{\min}$ remains limited; for instance, without s.h., $NF_{\min}$ (at 4.5 V) drops from 3.5 to 2.75 dB [12]. The voltage and frequency dependence of $NF_{\min}$ is described very well by both HD simulation and CM. DD and HD simulations showed that correlation between base and collector shot noise in the investigated LEC HBTs is fairly weak [37], particularly at relatively low frequencies (1 and 8 GHz), and thus was not analyzed in this paper.

The equivalent noise resistance (R_n) only slightly depends on V_{CE} and is well captured by CM, while HD simulation exhibits a somewhat weaker voltage dependence. According to Fig. 9, the magnitude of the optimum source reflection coefficient Γ_{OPT} is also described fairly well by both CM and HD device simulation. The latter shows a different trend, although at high voltages. For the phase of Γ_{OPT} in Fig. 10, CM yields excellent results up to about 4 V and then appears to increase more sharply than the measurement. HD simulation deviates at 8 GHz due to the missing parasitic substrate network but still exhibits a similar trend versus V_{CE} as measurement. In particular, at high V_{CE}, the increase is smaller than that of HICUM.

At this point, HD simulation has been verified as a reference model for investigating noise sources within a device. Therefore, it was used to obtain a feeling for the noise behavior up to the much higher frequency of 100 GHz. The corresponding data are shown in Fig. 11. A slight difference in $NF_{\min}$ is due to the missing external capacitances in the HD model mentioned earlier. However, the phase of Γ_{OPT} is quite sensitive to the external parasitic capacitance as shown in Fig. 12. CM simulations excluding the external capacitance portions yield results similar to those obtained from the HD model (cf. Fig. 12).

With the help of calibrated HD and CM, a decomposition of the impact of important effects on noise behavior was performed. The results of this analysis, as shown in Fig. 13, reveal that the main contribution to the increase in $NF_{\min}$ beyond about 2.5 V comes from II noise (curve 2). II noise itself is included in HICUM through the additional shot noise source, explaining the excellent agreement observed for the

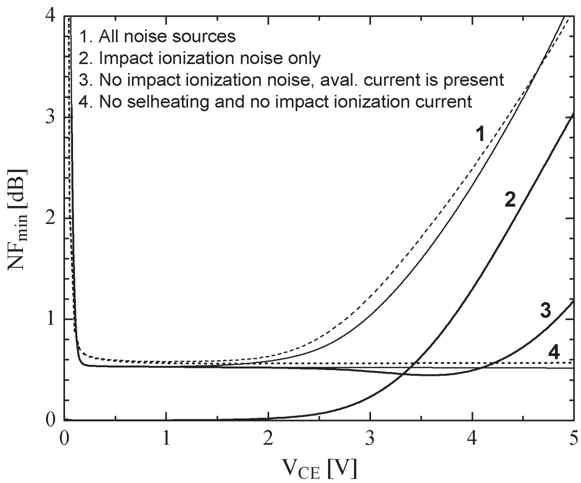

Fig. 13. Resolved noise sources for $NF_{\min}$ versus V_{CE} obtained from (solid lines) HICUM simulations at 1 GHz: (Curve 1) Complete model, (curve 2) noise from II only and no s.h., (curve 3) with avalanche effect and multiplication of shot noise but neglecting II noise, and (curve 4) neither II noise nor s.h. In addition, Galene results are inserted for cases 1 and 4.

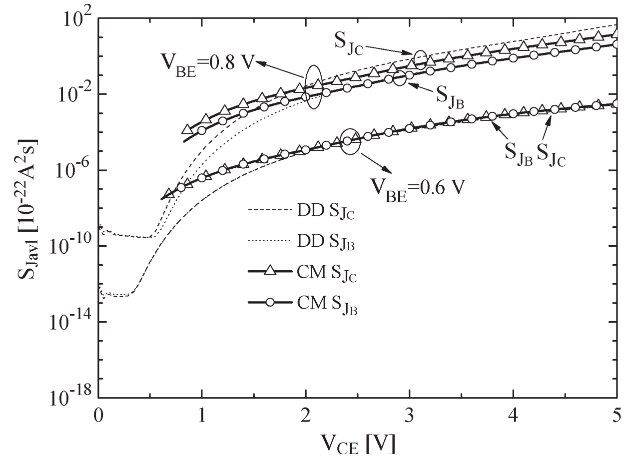

Fig. 14. Collector and base terminal current fluctuations due to II for two different V_{BE}: Comparison between DD device simulation (dashed lines) and HICUM (solid lines with symbols).

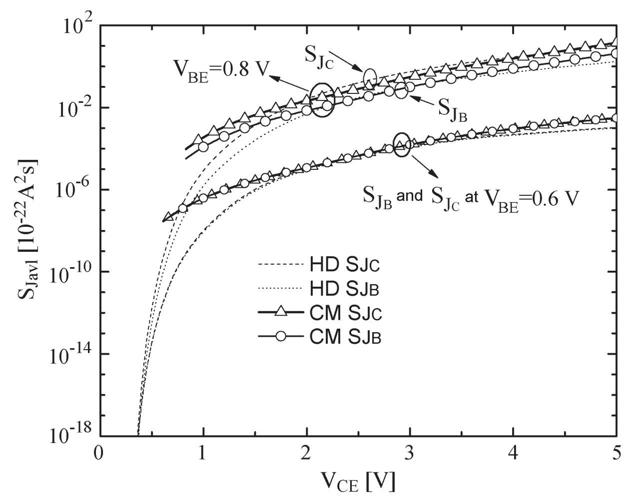

Fig. 15. Collector and base terminal current fluctuations due to II for two different V_{BE}: Comparison between HD device simulation (dashed lines) and HICUM (solid lines with symbols).

NPs shown before. Turning off the II noise source (in HICUM) only and keeping the II effect, the avalanche-multiplication-related collector shot noise amplification leads to a visible increase of $NF_{\min}$ (curve 3) at high V_{CE}, as was explained in [13]. Turning off the II effect completely in the models (curve 4) makes $NF_{\min}$ independent of V_{CE} [12]. Further decomposition of noise sources shows that the influence of thermal noise from the parasitic substrate resistance (R_{SU}) and of shot noise from the collector-substrate diode current on NPs is negligible as expected and, therefore, was neglected in the 2-D HD model.

The collector terminal excess noise, which is the part of the noise that exceeds the shot noise of the collector current without II, requires a more detailed investigation. For this, only the spectral densities S_{Javl} of the terminal current fluctuations due to II are analyzed with the help of HD and DD device simulations, in which the influence of s.h. and external parasitics were turned off. Due to the randomness of the II process, the avalanche current fluctuates, and an additional noise is introduced at both the collector and base terminals. The corresponding collector and base current fluctuations as a function of V_{CE} are shown in Fig. 14 for DD simulation and in Fig. 15 for HD simulation and are compared for both cases to CM. For all models, at $V_{\mathrm{BE}} = 0.8$ V $(J_C = 0.3\ \mathrm{mA}/\mu\mathrm{m}^2)$, the collector current and the base current fluctuations S_{Jc} and S_{Jb} can be clearly distinguished while they coincide at low injection (at $V_{\mathrm{BE}} = 0.6$ V, $J_C = 2.4^{*}10^{-4}\ \mathrm{mA}/\mu\mathrm{m}^2$). Generally, for constant V_{BE}, the hole current generated by the avalanche process consists of a component flowing across the BE junction and one through the base resistance to the base terminal. At low injection $(V_{\mathrm{BE}} = 0.6\ \mathrm{V})$, the avalanche current almost entirely flows through the base resistance to the base terminal. Therefore, the associated spectral density is the same as for the avalanche component at the collector terminal.

The comparison between DD and HD simulations in Figs. 14 and 15, respectively, reveals the biggest difference at low V_{CE}, which can be explained as follows. The DD model uses the local electric field to calculate the ionization coefficient, ignoring the fact that carriers need to acquire certain energy before they are able to ionize. This "threshold" behavior is captured more physically by HD simulation [31]. Therefore, the avalanche current from DD simulation is larger than the one from HD simulation, which uses a smaller nonlocal field. As a consequence, the II spectral densities are higher for DD than that for HD simulation. This is valid for the entire voltage range, although much more pronounced at low voltages.

Both Figs. 14 and 15 also contain HICUM results. At low V_{BE} and V_{CE} values beyond 2 V, excellent agreement is obtained with device simulation. In the HD case, the slight deviation in curvature toward high V_{CE} is caused by the difference in curvature for the M factor (cf. Fig. 3). This difference is not visible for the DD case, since the HICUM avalanche equation is based on the DD equations. Toward low voltages of V_{CE}, the avalanche-related spectral densities of CM remain higher than those from DD or HD device simulation. The reason for this is that the spatial dependence of the electric field in the CM avalanche expression is approximated only to the first order by the internal BC depletion capacitance. The lower the field (i.e., V_{CE}), the less accurate this description becomes. However, according to Fig. 3, below $V_{\mathrm{CE}} = 2$ V, the multiplication factor has dropped to such low values that the avalanche current is negligible anyway. Therefore, this inaccuracy of the CM is irrelevant for applications. Below $V_{\mathrm{CE}} = 2$ V, even noise (known as the most sensitive high-frequency figure of merit) is not affected by the presence of the II current ($NF_{\min}$ starts to increase only at $V_{\mathrm{CE}} > 2$ V). Therefore, the II approach in CM, based on the local field, is an acceptable solution for avalanche multiplication current noise modeling in SiGe HBTs. For higher V_{CE}, HICUM exhibits still the same trend as both DD and HD models. In both cases, the base-terminal-related spectral density portion of S_{Javl} agrees very well, while there are certain deviations for the collector-related portion.

IV. Conclusion

NPs as a function of CE voltage were investigated for 80-GHz LEC SiGe HBT with a special focus on the influence of II on noise in the base and collector current. HD and DD device simulations, calibrated by full-band MC solutions of the Boltzmann transport equation, were employed for gaining an understanding of the underlying device physics. For the first time, to our knowledge, II noise was simulated using HD and DD models and verified by experimental data over bias and frequency, establishing a basis for further detailed investigations of the fundamentals of HBT noise behavior, particularly at frequencies beyond existing equipment capability. For CM development purposes, experimental and device simulation data were verified against results obtained using weak avalanche-current approach, implemented in compact bipolar transistor model, in this particular case HICUM. Excellent agreement was obtained for all four NPs as a function of both frequency and V_{CE} as well as for dc and small-signal characteristics.

Detailed analysis of noise origin revealed that the strong increase of noise figure for voltages beyond BV_{CE0} is due to avalanche-current-related fluctuations itself rather than collector shot noise amplification or s.h. effects. The latter two effects lead only to a slight increase of noise figure. Carrier shot noise amplification due to avalanche multiplication impact is not the main contributor to $NF_{\min}$. The local field approach in HICUM is the reason for the multiplication factor deviation at low CE bias ($V_{\mathrm{CE}} < 1.5$ V). However, this does not cause significant deviations for the noise trend since II-related current fluctuations at such low voltages are rather small and thus negligible in $NF_{\min}$. Analysis of II noise spectral densities extracted from HD and DD simulations as well as from CM revealed that the CM formulation accurately describes II noise over the bias and frequency region of interest for present circuit applications.

Acknowledgment

The authors would like to thank F. Korndoerfer from IHP Frankfurt (Oder) for the experimental support and also S. Lehmann and A. Mukherjee for their help with HICUM parameter extraction and simulator usage.

References

[1] J. D. Cressler, *Silicon Heterostructure Handbook*. Boca Raton, FL: Taylor & Francis, 2006.

[2] J. S. Rieh, B. Jagannathan, H. Chen, K. T. Schoneberg, D. Angell, A. Chinthakindi, J. Florkey, F. Golan, D. Greenberg, S.-J. Jeng, M. Khater, F. Pagette, C. Schnabel, P. Smith, A. Stricker, K. Vaed, R. Volant, D. Ahlgren, G. Freeman, K. Stein, and S. Subbanna, "SiGe HBTs with cut-off frequency of 350 GHz," in *IEDM Tech. Dig.*, 2002, pp. 771–774.

[3] J.-S. Rieh, B. Jagannathan, D. R. Greenberg, M. Meghelli, A. Rylyakov, F. Guarin, Z. Yang, D. C. Ahlgren, G. Freeman, P. Cottrell, and D. Harame, "SiGe heterojunction bipolar transistors and circuits toward terahertz communication applications," *IEEE Trans. Microw. Theory Tech.*, vol. 52, no. 10, pp. 2390–2408, Oct. 2004.

[4] B. Heinemann, R. Barth, D. Bolze, J. Drews, P. Formanek, T. Grabolla, U. Haak, W. Höppner, D. Knoll, B. Kuck, R. Kurps, K. Köpke, S. Marschmeyer, H. Rücker, H. H. Richter, P. Schley, D. Schmidt, W. Winkler, D. Wolansky, H.-E. Wulf, and Y. Yamamoto, "Novel collector design for high-speed SiGe: C HBTs," in *IEDM Tech. Dig.*, 2002, pp. 775–778.

[5] J. Yuan, R. Krithivasan, J. D. Cressler, M. H. Khater, D. C. Ahlgren, and A. J. Joseph, "On the frequency limits of SiGe HBTs for TeraHertz applications," in *Proc. IEEE BCTM*, 2007, pp. 22–25.

[6] P. Chevalier, B. Barbalat, L. Rubaldo, B. Vandelle, D. Dutartre, P. Bouillon, T. Jagueneau, C. Richard, F. Saguin, A. Margain, and A. Chantre, "300 GHz $f_{\max}$ self-aligned SiGeC HBT optimized towards CMOS compatibility," in *Proc. IEEE BCTM*, 2005, pp. 120–123.

[7] T. Kimura, "Factors affecting fiber-optic transmission quality," *J. Lightw. Technol.*, vol. 6, no. 5, pp. 611–619, May 1988.

[8] H. M. Rein, R. Schmid, P. Weger, T. Schmith, T. Herzog, and R. Lachner, "A versatile Si-bipolar driver circuit with high output voltage swing for external and direct laser modulation in 10 Gb/s optical-fiber links," *IEEE J. Solid-State Circuits*, vol. 29, no. 9, pp. 1014–1021, Sep. 1994.

[9] M. Rickelt, H.-M. Rein, and E. Rose, "Influence of impact-ionization-induced instabilities on the maximum usable output voltage of Si-bipolar transistors," *IEEE Trans. Electron Devices*, vol. 48, no. 4, pp. 774–783, Apr. 2001.

[10] J. Kraft, D. Kraft, B. Löfler, H. Jauk, and E. Wachmann, "Usage of HBTs beyond $\mathrm{BV_{CE0}}$," in *Proc. IEEE BCTM*, 2005, pp. 33–36.

[11] D. R. Greenberg, S. Sweeney, G. Freeman, and D. Ahlgren, "Low-noise performance near $\mathrm{BV_{CE0}}$ in a 200 GHz SiGe technology at different collector design points," in *Proc. IEEE MTT-S IMS Dig.*, 2003, pp. 113–116.

[12] M. Ramonas, C. Jungemann, P. Sakalas, M. Schroter, and W. Kraus, "Microscopic modeling of impact-ionization noise in SiGe heterojunction bipolar transistors," in *Proc. SPIE Conf. Noise Fluctuations Circuits Mater.*, M. Maccuci, L. K. J. Vandamme, C. Ciofi, and M. B. Weissman, Eds. Bellingham, WA: SPIE, 2007, vol. 6600, p. 660 01F.

[13] J. C. J. Paasschens and R. de Krot, "Modeling the excess noise due to avalanche multiplication in (hetero-junction) bipolar transistors," in *Proc. IEEE BCTM*, 2004, pp. 108–111.

[14] R. J. McIntyre, "Multiplication noise in uniform avalanche diodes," *IEEE Trans. Electron Devices*, vol. ED-13, no. 1, pp. 164–168, Jan. 1966.

[15] J. C. Marsland, "On the effect of ionization dead spaces on avalanche multiplication and noise for uniform electric fields," *J. Appl. Phys.*, vol. 67, no. 4, pp. 1929–1933, Feb. 1990.

[16] M. M. Hayat, W. L. Sargeant, and B. E. A. Saleh, "Effect of dead space on gain and noise in Si and GaAs avalanche photodiodes," *IEEE J. Quantum Electron.*, vol. 28, no. 5, pp. 1360–1363, May 1992.

[17] R. J. McIntyre, "A new look at impact ionization—Part I: A theory of gain, noise, breakdown probability, and frequency response," *IEEE Trans. Electron Devices*, vol. 46, no. 8, pp. 1623–1631, Aug. 1999.

[18] E. Crabbe, J. Stork, G. Baccarani, M. Fischetti, and S. Laux, "The impact of non-equilibrium transport on breakdown and transit time in bipolar transistors," in *IEDM Tech. Dig.*, 1990, pp. 463–466.

[19] P. Yuan, K. A. Anselm, C. Hu, H. Nie, C. Lenox, A. L. Holmes, B. G. Streetman, J. C. Campbell, and R. J. McIntyre, "A new look at impact ionization—Part II: Gain and noise in short avalanche photodiodes," *IEEE Trans. Electron Devices*, vol. 46, no. 8, pp. 1632–1639, Aug. 1999.

[20] C. C. McAndrew, J. A. Seitchik, D. F. Bowers, M. Dunn, M. Foisy, I. Getreu, M. McSwain, S. Moinian, J. Parker, D. J. Rouston, M. Schroter, P. van Wijnen, and L. F. Wagner, "VBIC95, the vertical bipolar inter-company model," *IEEE J. Solid-State Circuits*, vol. 31, no. 10, pp. 1476–1483, Oct. 1996.

[21] M. Schroter, "High-frequency circuit design oriented compact bipolar transistor modeling with HICUM: Analog circuit and device technologies," *IEICE Trans. Electron.*, vol. E88-C, no. 6, pp. 1098–1113, 2005.

[22] J. C. J. Paasschens and W. J. Kloosterman, "The Mextram bipolar transistor model," Philips Nat. Lab., Redhill, U.K., Unclassified Report NL-UR 2000/811, 2000. level 504.
[23] J. Berkner, "Compact models for bipolar transistors," in *Proc. Eur. IC-CAP Device Model, Workshop*, Berlin, Germany, Mar. 7–8, 2002, p. 17.
[24] A. Schüppen, M. Totschanoff, J. Berntgen, P. Maier, D. Zerrweck, H. von der Ropp, J. Tolonics, and K. Burger, "The proliferation of silicon germanium," in *Proc. ESSDERC*, 2000, pp. 88–91.
[25] [Online]. Available: http://www.atmel.com
[26] J. Berntgen, A. Schueppen, P. Maier, M. Tortschanoff, W. Kraus, and M. Averweg, "SiGe technology bears fruits," *Mater. Sci. Eng. B*, vol. 89, no. 1, pp. 13–20, Feb. 2002.
[27] M. C. A. Koolen, J. A. M. Geelen, and M. P. J. G. Versleijen, "An improved de-embedding technique for on-wafer high-frequency characterization," in *Proc. IEEE BCTM*, 1991, pp. 188–191.
[28] H. Hillbrand and P. H. Russer, "An efficient method for computer aided noise analysis of linear amplifier networks," *IEEE Trans. Circuits Syst.*, vol. CAS-23, no. 4, pp. 235–238, Apr. 1976.
[29] B. Neinhus, S. Decker, P. Graf, F. M. Bufler, and B. Meinerzhagen, "Consistent hydrodynamic and Monte-Carlo simulation of SiGe HBTs based on table models for the relaxation times," *VLSI Des.*, vol. 8, no. 1–4, pp. 387–391, 1998.
[30] C. Jungemann, S. Keith, and B. Meinerzhagen, "Full-band Monte Carlo device simulation of a Si/SiGe-HBT with a realistic Ge profile," *IEICE Trans. Electron.*, vol. E83-C, no. 8, pp. 1228–1234, 2000.
[31] C. Jungemann, B. Meinerzhagen, S. Decker, S. Keith, S. Yamaguchi, and H. Goto, "Is physically sound and predictive modeling of NMOS substrate currents possible?" *Solid State Electron.*, vol. 42, no. 4, pp. 647–655, Apr. 1998.
[32] R. K. Mains, G. I. Haddad, and P. A. Blakey, "Simulation of GaAs IMPATT diodes including energy and velocity transport equations," *IEEE Trans. Electron Devices*, vol. ED-30, no. 10, pp. 1327–1337, Oct. 1983.
[33] M. Schroter, H.-M. Rein, W. Rabe, R. Reimann, H.-J. Wassener, and A. Koldehoff, "Physics- and process-based bipolar transistor modeling for integrated circuit design," *IEEE J. Solid-State Circuits*, vol. 34, no. 8, pp. 1136–1149, Aug. 1999.
[34] G. Niu, J. D. Cressler, S. Zhang, U. Gogineni, and D. Ahlgren, "Measurement of collector-base junction avalanche multiplication effects in advanced UHV/CVD SiGe HBTs," *IEEE Trans. Electron Devices*, vol. 49, no. 5, pp. 1007–1015, May 1999.
[35] M. Schroter, Z. Yan, T.-Y. Lee, and W. Shi, "A compact tunneling current and collector breakdown model," in *Proc. IEEE BCTM*, Minneapolis, MN, 1998, pp. 203–206.
[36] C. Jungemann, B. Neinhus, and B. Meinerzhagen, "Hierarchical 2-D DD and HD noise simulations of Si and SiGe devices—Part I: theory," *IEEE Trans. Electron Devices*, vol. 49, no. 7, pp. 1250–1257, Jul. 2002.
[37] M. Ramonas, P. Sakalas, C. Jungemann, M. Schroter, W. Kraus, and A. Shimukovitch, "Microscopic modeling of high frequency noise in SiGe HBTs," in *Proc. 37th ESSDERC*, Munich, Germany, Sep. 11–13, 2007, pp. 183–186.

Paulius Sakalas received the Ph.D. degree in physics and mathematics from Vilnius State University, Vilnius, Lithuania, in 1990.

In 1983, he joined the Fluctuation Phenomena Laboratory, Semiconductor Physics Institute, Lithuanian Academy of Sciences, Vilnius. In 1991, he was a Quest Research with Eindhoven University of Technology, Eindhoven, The Netherlands. In 1996 and 1997, he was a Visiting Scientist with the Physical Electronics and Photonics and Microwave Laboratories, Chalmers University of Technology, Gothenburg, Sweden. During 1998–1999, he was a Guest Research with CNET France Telecom, Grenoble, France. During 1999–2000, he joined the Microwave Electronics Laboratory, Chalmers University of Technology, where he worked on high-frequency noise in MOSFETs, pHEMTS, and MMICs. He is currently a Head Scientist with the Fluctuation Phenomena Laboratory, Semiconductor Physics Institute, and a Senior Researcher with the Institute of Electrical Engineering and Electronics, Dresden University of Technology, Dresden, Germany. His research interests include high-frequency noise, load pull measurements, compact and device level modeling of microwave and low-frequency noise, and power characteristics in SiGe, AIIIBV HBTs, HEMTs, MOSFETs, and LNAs.

Mindaugas Ramonas received the M.S. and Ph.D. degrees in physics from Vilnius University, Vilnius, Lithuania, in 1998 and 2003, respectively.

Since then, he has been a Research Fellow with the Fluctuation Research Laboratory, Semiconductor Physics Institute, Vilnius, Lithuania. He is currently on leave from Bundeswehr University München, Münich, Germany. His research interests include Monte Carlo modeling of electron transport and noise in semiconductor materials and numerical device modeling.

Michael Schröter (M'93–SM'08) received the Dipl.-Ing. and Dr.-Ing. degrees in electrical engineering and the "venia legendi" in semiconductor devices from the Ruhr-University Bochum, Bochum, Germany, in 1982, 1988, and 1994, respectively.

From 1993 to 1996, he was with Nortel and Bell Northern Research, Ottawa, ON, Canada, where he was first a Senior Member of the Scientific Staff and later as Team Leader and Advisor, continuing the bipolar-transistor modeling and parameter extraction activities. From 1994 to 1996, he was an Adjunct Professor with Carleton University, Ottawa. In 1996, he was with Rockwell Semiconductor Systems, Newport Beach, CA, where he established and managed the RF Device Modeling Group and was responsible for modeling (Si, SiGe, and AlGaAs) bipolar transistors, MOS transistors, and integrated passive devices with emphasis on high-frequency process technologies and applications. Since 1999, he has been a Full Professor with Dresden University of Technology, Dresden, Germany. He has also been an Adjunct Research Professor with the University of California, San Diego, La Jolla. He is also currently the Technical Program Manager of DOTFIVE, an EU FP7 Integrated Project on 0.5-THz SiGe HBT technology development. He is a Cofounder of XMOD Technologies, a company specializing in high-frequency semiconductor-device modeling services for foundries and design houses. He also serves on the Technical Advisory Boards of RFMagic (currently Entropic Inc.), a communications circuit-design company in San Diego, CA, and of RFNano, a start-up company in Irvine, CA. He has published about 100 technical papers and contributed several book chapters. He has also given numerous lectures and invited tutorials on compact device modeling at international conferences and industrial sites. He is a regular Reviewer for internationally renowned scientific journals. He is the author of the compact bipolar-transistor-model HICUM, which has been an industry-wide standard for several years.

Prof. Schröter was a member of the CAD/Modeling subcommittee of the IEEE Bipolar/BiCMOS Circuits and Technology Meeting from 1994 to 2001, which he chaired from 1998 to 2000. More recently, he has been serving on the organizing committee of the IEEE Workshop on Compact Modeling for RF/Microwave Applications and of the Semiconductor Conference Dresden.

Christoph Jungemann (M'97–SM'06) received the Dipl.-Ing. and Dr.-Ing. degrees in electrical engineering from the Technical University of Aachen (RWTH Aachen), Aachen, Germany, in 1990 and 1995, respectively, and the "venia legendi" in "Theoretische Elektrotechnik" from the University of Bremen, Bremen, Germany, in 2001.

From 1990 to 1995, he was a Research and Teaching Assistant with the "Institut für Theoretische Elektrotechnik," RWTH Aachen. From 1995 to 1997, he was with the Research and Development Facility, Fujitsu Limited, Kawasaki, Japan. From 1997 to 2002, he was a Chief Engineer with the "Institut für Theoretische Elektrotechnik und Mikroelektronik," University of Bremen. From 2002 to 2003, he spent a one-year sabbatical with the Center for Integrated Systems, Stanford University, Stanford, CA. From 2003 to 2006, he was a Research Associate with the Technical University of Braunschweig, Braunschweig, Germany. Since 2006, he has been a Full Professor of microelectronics with Bundeswehr University München, Münich, Germany. His main research interests include full-band Monte-Carlo simulation of Si and SiGe devices, numerical device modeling, transport in inversion layers, and noise modeling.

Prof. Jungemann is a member of the Board of Editors of the IEEE TRANSACTIONS ON ELECTRON DEVICES and has served on the technical program committees of the International Workshop on Computational Electronics, the International Electron Devices Meeting, and the International Conference on Computer-Aided Design. He was the corecipient of the IEEE EDS Paul Rappaport Award in 2005.

Artur Shimukovitch was born in Vilnius, Lithuania, in 1974. He received the B.S. degree in physics from Vilnius Pedagogical University, Vilnius, in 2003 and the M.S. degree in engineering informatics from Vilnius Gediminas Technical University, Vilnius, in 2005. He is currently working toward the Ph.D. degree in semiconductor device physics at the Semiconductor Physics Institute, Vilnius.

In 2003, he joined the Fluctuation Phenomena Laboratory, Semiconductor Physics Institute. His research interests include compact modeling and high-frequency noise, and power investigation in SiGe, AIIIBV HBTs, GaN FETs, and MOSFETs.

Wolfgang Kraus (M'83–SM'01) received the M.S. and Ph.D. degrees in electrical engineering from the University of Saarland, Saarbrücken, Germany, in 1982 and 1988, respectively. His M.S. thesis was on parameter extraction for BJTs. His Ph.D. thesis was on numerical methods for RF-noise modeling of semiconductor devices.

From 1982 to 1984, he worked on integrated circuit design for Philips (Nuremberg, Germany) and BOSCH (Reutlingen, Germany). Since 1988, he has been with Atmel (formerly TEMIC), Heilbronn, Germany, where he worked on integrated circuit design during 1990–1993, computer-aided design (CAD) during 1994–1998, and modeling for circuit design during 1988–1990. Since 1998, he has been working on circuit design modeling. During the time of his CAD activities, he was one of the main contributors to a mixed-signal simulator built on top of ELDO from ANACAD/Mentor Graphics.

Dr. Kraus is a member of the German Association for Electrical, Electronic & Information Technologies (VDE). He was also the representative of Atmel in the Compact Model Council from 2000 to 2008 and from 2004 to 2008 in the modeling subcommittee of the IEEE Bipolar/BiCMOS Circuits and Technology Meeting (BCTM).